other known approaches, ML and MBF, has shown that the performance of LQSC is much higher than that of ML. The performance of LQSC is slightly lower than that of MBF, although the control logic is simpler than that of MBF. It should be noted that, as shown in Ref. 3, the system with any of these approaches is always stable because it is the type-II variable-stiffness system.

References

[1]Chen, J.-C., "Response of Large Space Structures with Stiffness Control," *Journal of Spacecraft and Rockets*, Vol. 21, No. 5, 1984, pp. 463–467.

[2]Fanson, J. L., Chen, J.-C., and Caughey, T. K., "Stiffness Control of Large Space Structures, Control of Flexible Space Structures," Jet Propulsion Lab., JPL Publication 85-29, California Inst. of Technology, Pasadena, CA, April 1985, pp. 351–364.

[3]Onoda, J., Endo, T., Tamaoki, H., and Watanabe, N., "Vibration Suppression by Variable-Stiffness Members," *AIAA Journal*, Vol. 29, No. 6, 1991, pp. 977–983.

[4]Minesugi, K., "Vibration Control of Flexible Structures by Variable Axial Stiffness Active Members," Ph.D. Dissertation, Dept. of Aeronautics, Univ. of Tokyo, Japan, Dec. 1990 (in Japanese).

[5]Kwakernaak, H., and Sivan, R., *Linear Optimal Control System*, Wiley-Interscience, New York, 1972.

Structure and Properties of Three-Dimensional Braided Composites Including Axial Yarns

Soheil Mohajerjasbi*
Boeing Defense and Space Group, Philadelphia, Pennsylvania 19142-0858

Introduction

TEXTILE preforming and resin transfer molding (RTM) have been identified among the manufacturing processes that offer the potential to make composite structures cost effective compared with aluminum structures. The potential of textile composites in reducing cost is envisioned in the ability to manufacture near-net-shape parts and the use of fiber and matrix in their lowest cost form. The cost-saving potential of textile composites is realized when the process of preform fabrication is automated and therefore the labor-intensive process of laying up the laminate or the dry fabric by hand is eliminated.

One such textile preforming process is three-dimensional Cartesian braiding that produces three-dimensional preform. A wide range of complex geometric shapes may be produced by this process. Other advantages of this class of composites include delamination resistance and good energy absorption capability. The process is not without limitations, however; presently available braiding machines are not fully automated, are relatively slow, and the size of the parts that can be produced with this process is limited by the physical dimensions of the braiding machine.

Any attempt to model the thermoelastic properties of this class of composites should take into account the structure of the preform, which is much different from the conventional laminated composites.

Fiber Architecture

A braiding machine, schematically shown in Fig. 1, is used to fabricate three-dimensional braided preforms. The yarn carriers that

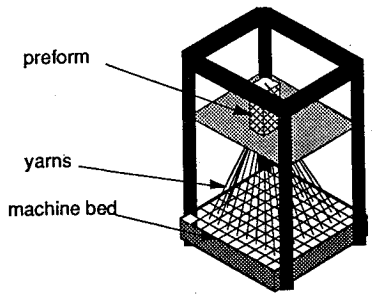

Fig. 1 Schematic of a three-dimensional Cartesian braiding machine.

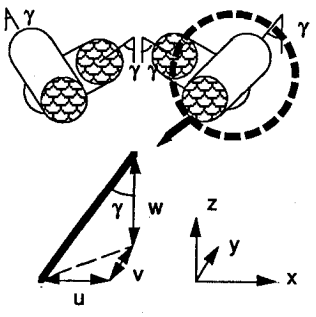

Fig. 2 Yarn arrangement in the interior of three-dimensional braided composite.

are loaded with yarns are arranged in rows and columns on the machine bed to form a shape similar to the shape of the preform to be produced. The ends of the yarns are tied to a movable plate above the braiding machine. Movements of the yarn carriers on the machine bed in a prescribed manner will produce the braided preform above the machine. The number, arrangement, and the movements of the yarn carriers on the machine bed determine the fiber architecture of the preform. The braiding process that is considered here is referred to as (1 × 1) or four-step process. In the four-step process, similar yarn carrier configuration is obtained after every four machine steps, and therefore the fiber architecture of the preform is a repetition of the fiber architecture produced in four machine steps. This yarn structure is referred to as repeat unit. It is possible to add stationary yarns on the machine that do not participate in these carrier movements. These yarns will remain parallel to the braiding axis, and the resulting preform will have axial yarns that are directed along the length of the preform.

In the following, the fiber architecture of the repeat unit is briefly reviewed. More detailed explanation of the yarn carrier movements and the resulting fiber architecture of the preform may be found in Ref. 1.

In every two machine steps, as a result of the movements of the yarn carriers on the bed of the braiding machine, the yarns in the interior of the preform produce two different yarn formations that are characterized by interior braiding angle γ with respect to the axis of the braided preform (z axis). These two yarn formations, which are shown in Fig. 2, are not identical, but a symmetry exists between them. These two yarn formations alternate along 45 and 135 deg measured from the preform x axis and along the axis of the braided preform (z axis). The movements of the carriers resulting in formation of the boundary and corners are different; therefore the fiber architectures at the corners and the boundaries are different from the interior. The fiber architectures at the boundaries and corners of the preform are also demonstrated in Ref. 1. The interior braiding angle γ cannot be measured directly without cutting the preform; however, it can be calculated from orientation angle of the yarns on the surface of the composite, which is referred to as surface angle. A relationship exists between the interior braiding angle, the surface angle, and the parameters u, v, and w shown in Fig. 2. Equations establishing the relationship between the interior braiding angle, the surface angle, and the parameters u, v, and w may be found in Refs. 1 and 2.

The three parameters u, v, and w completely describe the geometry of the interior, boundaries and the corners of the preform. Since the fiber architecture of the preform is the repeat of the yarn

Received Feb. 13, 1995; revision received Sept. 5, 1995; accepted for publication Sept. 14, 1995.

*Staff Engineer, Helicopters Division, P.O. Box 16858, MS P38-13. Member AIAA.

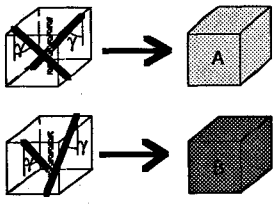

Fig. 3 Interior yarn formations shown as type A and type B interior cells.

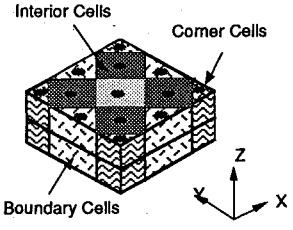

Fig. 4 Schematic of the FE model.

structure formed during four machine step, these three parameters and the number and arrangement of yarn carriers on the machine bed completely describe the fiber architecture of the preform. In the case of braided preforms with axial yarns, the axial yarns will be oriented parallel to the z axis.

The fiber architecture of the braided composite including the axial yarns may be better demonstrated if the two interior yarn formations (Fig. 2), after consolidation with matrix material, are represented as type A and type B interior cells, as shown in Fig. 3.

In Fig. 3, the dark lines represent the braiding yarns (shrunk in size to avoid clutter), and the cubical shapes represent the matrix material that encapsulates these yarns. The axial yarns are represented as the lines with light shading. Now, using these definitions for the two types of interior cells and including the boundary and corner cells, the repeat unit of the braided composite with four yarn carriers on each side may be represented as shown in Fig. 4.

Analysis Method

Different approaches have been taken in the existing analytical models to predict the mechanical behavior of three-dimensional braided composites. Most of these models, which are briefly reviewed in Ref. 3, are based on an idealized unit cell and do not account for the differences in fiber architecture in the interior, boundaries, and the corners.

In the present approach a finite element based method is used to calculate the elastic constants of three-dimensional braided composite. One repeat unit of the composite, which is considered to represent the properties of the braided composite as a whole, is used for modeling. A schematic of the finite element (FE) model, which represents the repeat unit of a three-dimensional braided composite with four yarns on each side of the section, is shown in Fig. 4. The previously introduced convention of type A and type B cells, shown in Fig. 3, is observed, and the boundary and corner cells are also added. It should be noted that the yarns and the matrix are not smeared as is customary in modeling composite materials but are modeled distinctly. The dark spots represent the intersection of the axial yarns with the upper plane of the repeat unit, whereas the braiding yarns in the interior, boundaries, and corners are not shown to avoid clutter. The geometry of the model is defined by grids on three planes that correspond to the lower, middle, and the upper planes of the repeat unit and represent the corner points of the type A and type B interior cells, and the boundary and corner cells. The coordinates of these grids are completely described by the parameters u, v, and w, which may be measured from the surfaces of the composite when modeling a specific specimen. For parametric studies, however, the dimensions of the cells may be normalized with respect to u. Then by changing the normalized height of the cells, which is the z coordinates of the grids on the middle and top planes, different interior braiding angles are simulated. Also, from the knowledge of the total length of the yarns in the repeat unit, which is a function of the interior braiding angle, and the total dimensions of the repeat unit, areas may be calculated for the yarns in the model to result in the desired fiber volume fraction. MSC/NASTRAN finite element code is used to model the structure of the repeat unit. The yarns are modeled using axial elements with axial stiffness only (ROD). The transverse properties of impregnated yarn are calculated from a rule of mixture and assigned to the matrix. Moreover, since the space occupied by the axial elements is also occupied by the matrix, the axial properties of the yarns are modified to avoid double counting. The matrix is modeled using solid elements (HEXA, and PENTA) with isotropic properties. Multipoint constraint equations (MPC) are written to tie the degrees of freedom at the ends of the axial elements, which represent the braiding and axial yarns, to their corresponding points on the solid elements, which represent the matrix. It should be pointed out that by treating the three-dimensional braided composite in this manner, displacement compatibility between the axial elements and the solid elements only exist at the endpoints of the axial elements and not at any other intermediate point along their length. Also, even though the overall Poisson's effect is believed to be simulated, no interface effects between the yarn and the matrix are accounted for.

The FE model obtained in this manner is constrained to remove the rigid-body motion, and different boundary conditions are applied to calculate the different average elastic constants of the braided composite. For example, to calculate the average longitudinal modulus in any direction, the nodes on one face of the model are constrained in that direction only, and the nodes on the opposite face are displaced by the amount needed to produce a unit strain in that direction. The forces of constraint on the nodes of the displaced face of the model

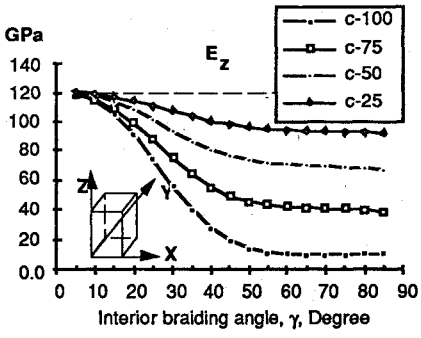

a) Axial modulus, z direction

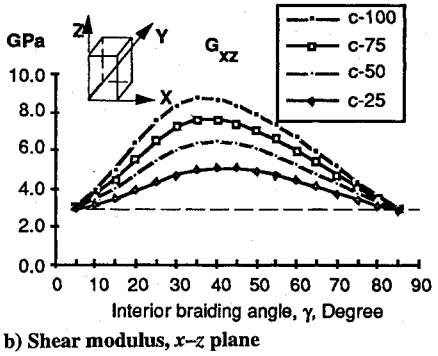

b) Shear modulus, x–z plane

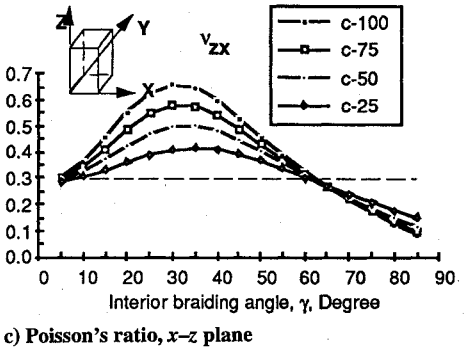

c) Poisson's ratio, x–z plane

Fig. 5 Elastic properties of a square braided GR/E composite as a function of different percentage of axial yarns: GR/E V_f = 0.50; c-100 = 100% braided, 0% axials; c-75 = 75% braided, 25% axials; c-50 = 50% braided, 50% axials; and c-25 = 25% braided, 75% axials.

are summed up and divided by the area of that face of the model to find the average applied stress. Since a unit strain is applied, the calculated average stress represents the longitudinal modulus in that direction. Similarly, to calculate the shear moduli of the composite, displacements are applied to the nodes on four faces to produce a unit shear strain. For example, to calculate G_{xy}, in-plane displacements in the x and y directions are imposed on the left, right, front, and back faces as a function of their coordinates (x, y) and with the proper sign to produce a unit shear strain. Summation of forces of constraint in the y direction on the right face is found and divided by the area of that face to calculate average shear stress. Since a unit shear strain is applied, the calculated average shear stress represents the shear modulus in that plane. Poisson's ratios are found by calculating the average transverse strain due to a unit strain in the primary direction.

Using this FE model, predictions were made for the engineering constants as a function of different percentages of axial yarns and interior braiding angle for a 50% fiber volume fraction graphite/epoxy (GR/E) braided composite. Some of these predictions are shown in Fig. 5, whereas the remaining constants are presented in Ref. 2. Values of 34.0 Msi (234.4 GPa) and 0.5 Msi (3.4 GPa) were used for the moduli of the graphite yarn and epoxy matrix, respectively. The straight dashed lines in these figures represent the expected unidirectional properties for a composite with similar fiber volume fraction.

A few observations may be made based on the information in Fig. 5.

1) The percentage of axial yarns has a pronounced effect on the axial modulus and the shear modulus in the x–z plane.

2) As the interior braiding angle becomes small, the braiding yarns line up with the z axis (see Fig. 2) and the braided composite resembles a unidirectional composite. With decreasing values of interior braiding angle, the predictions of the model for all axial yarn percentages converge to approximately the same point, which represents the properties of a unidirectional composite with the same fiber volume fraction.

3) With increasing percentage of axial yarns, all of the elastic properties approach the dashed line, which represents the properties of a unidirectional material. At this limit all properties become independent of the interior braiding angle.

4) The three-dimensional braided composite may exhibit relatively large values of Poisson's ratio ν_{zx}.

Observations 2 and 3 just stated demonstrate that the predictions of the model follow the expected trends in those limiting cases.

To demonstrate the predicting capability of this technique, a few specimens were prepared from a braided panel provided by Atlantic Research Corp. and tested in simple tension. Good correlation was found between the test results and the predictions of the model. Specimen specifications and test results are summarized in Ref. 2.

References

[1]Mohajerjasbi, S., "Structure and Mechanical Properties of 3-D Braided Composites," Ph.D. Thesis, Dept. of Mechanical Engineering, Drexel Univ., Philadelphia, PA, July 1993.

[2]Mohajerjasbi, S., "Modeling and Analysis of 4-Step 3-D Cartesian Braided Composites Including Axial Yarns," *Proceedings of the AIAA/ASME/ASCE/AHS/ASC 36th Structures, Structural Dynamics, and Materials Conference* (New Orleans, LA), AIAA, Washington, DC, 1995, pp. 8–16 (AIAA Paper 95-1157).

[3]Mohajerjasbi, S., "Analytical Models for Prediction of Thermoelastic Properties of 3-D Braided Composites—A Review," *Innovative Processing and Characterization of Composite Materials*, edited by R. F. Gibson, T. W. Chou, and P. K. Raju, American Society of Mechanical Engineers, New York, 1995, pp. 329–342.